D. Goldie, J. Landon, *Br. Med. Bull.* **38** (1974); D. B. Cottrell, E. C. Toren, Jr., J. A. Magnuson, S. J. Updike, *Clin. Chem.* **21**, 829 (1975); A. Pollard and C. B. Waldron, in *Automation in Analytical Chemistry* (Mediad, White Plains, N.Y., 1967); T. Marschner, F. Erhardt, J. Henner, P. C. Scriba, *Z. Klin. Chem. Klin. Biochem.* **13Jg**, 481 (1975).
3. Patent has been applied for by University of Virginia.
3a. We are currently performing all of our routine radioimmunoassays with the Gammaflow system at a rate of 35 samples per hour and an incubation time of 2 to 7 minutes at room temperature.
4. T. W. Smith, V. P. Butler, E. Haber, *N. Engl. J. Med.* **281**, 1212 (1969).
5. A. L. Steiner, D. M. Kipnis, R. Utiger, C. W. Parker, *Proc. Natl. Acad. Sci. U.S.A.* **64**, 367 (1969).
6. J. F. Harper and G. Brooker, *J. Cyclic Nucleotide Res.* **1**, 207 (1975).
7. T. L. Goodfriend, D. L. Ball, D. B. Farley, *J. Lab. Clin. Med.* **72**, 648 (1968).
8. M. Hufner and R. D. Hesch, *Acta Endocrinol.* **72**, 464 (1973).
9. P. R. Larsen, J. Dockalova, D. Sipula, F. M. Wu, *J. Clin. Endocrinol. Metab.* **37**, 177 (1973).
10. S. A. Berson and R. S. Yalow, *J. Clin. Invest.* **38**, 1996 (1959).
11. G. Brooker and R. W. Jelliffe, *Circulation* **45**, 20 (1972).
12. Corning Immophase T4 RIA and Roche T4 RIA published test kit data.
13. C. R. Morgan and A. Lazarow, *Diabetes* **12**, 115 (1963).
14. We thank Dr. Carlos Ayers for providing the serum samples and test results obtained on these serum samples when assayed by the Burroughs-Wellcome digoxin radioimmunoassay test kit.
15. T. W. Smith and K. M. Skubitz, *Biochemistry* **14**, 1496 (1975).
16. We thank Dr. T. W. Smith for the antiserum to digoxin, Dr. F. Murad for the antiserum to cyclic GMP, Dr. Sidney Hess for the antiserum to cyclic AMP, and Dr. Ted Goodfriend for the antiserum to angiotensin I. The antiserum to insulin was purchased from New England Nuclear and the antiserum to thyroxine from Calbiochem. We thank Dr. Robert Wilson and Dr. Gerald Cook for their interest in this project, C. Harding for preparing the pictorial representations of the system, and to R. Moylan for programming the H-P 9815 computer. Supported by NIH Diabetes-Endocrinology Research Center grant AM 17042 and NIH grant HL 15985, PHS career development award HL 00098 to G.B. and NIH postdoctoral fellowship HL 01320 to W.L.T.

Picosecond Chemistry

A variety of ultrafast molecular processes have been measured by picosecond spectroscopic techniques.

G. E. Busch and P. M. Rentzepis

Intense light pulses with a duration of a few picoseconds (10^{-12} second) generated by mode-locked lasers were first utilized for studies of ultrafast physical and chemical processes (*1*) in 1967. Since then, there has been a tremendous growth in the number and variety of experiments being conducted by picosecond spectroscopic techniques. These experiments have led to more sensitive and refined data; for example, the 1967 7-psec value for the relaxation time of azulene had been reduced to 4 psec by 1974 (*2*). Although a large number of research groups are actively engaged in investigations of ultrafast phenomena by picosecond methods, only a small number are directly involved in measuring chemical interactions.

A partial list of general research areas in chemistry in which picosecond spectroscopy has been used to probe ultrafast molecular processes includes: (i) vibrational relaxation within the ground electronic states of small molecules and within the excited states of large molecules; (ii) rates of internal conversion between singlet molecular electronic states and of intersystem crossing between singlet and triplet states; (iii) orientational relaxation rates of large molecules in solution; (iv) the dynamics of the trapping and solvation of excess electrons; (v) fast relaxation processes in excited laser dye molecules; (vi) cage effects on chemical reactions in solution; and (vii) primary events in vision and photosynthesis. Several investigators (*3*) have reviewed the work that had been done in these and other areas of ultrafast measurements up to 1974. We will not attempt here to present a comprehensive treatment of all the research that has been conducted since that time, but instead we will discuss progress in several areas that have been of particular interest to us. We begin with a brief description of some experimental techniques commonly used in picosecond studies.

Experimental Method

Numerous variations in experimental arrangements can be used to acquire data on ultrafast processes (*2–4*). The choice of a suitable configuration depends as much on individual preference as on the wavelength, intensity, and resolution requirements imposed by a particular experiment. A typical time-resolved picosecond spectroscopy experiment consists of (i) the irradiation of a sample with a laser pulse having a duration of a few picoseconds, (ii) probing of the sample before, during, and after excitation, and (iii) acquisition and analysis of experimental data. A general experimental configuration used to carry out these operations is illustrated schematically in Fig. 1. In the majority of our experiments, the laser system consists of a neodymium-doped glass oscillator and amplifier. The oscillator produces a train of about 100 infrared light pulses separated by the round-trip transit time of light in the laser cavity. Each pulse contains about 1 millijoule of energy at 1.06 micrometers and has a full width at half maximum of 5 to 10 psec.

For most experiments a single pulse is selected from the train and amplified to ~ 50 millijoules. The infrared pulse may be used directly to irradiate the sample or may be frequency-shifted by various nonlinear techniques such as harmonic generation or stimulated Raman scattering to produce excitation at other wavelengths. In addition, various probe pulses or shuttering pulses, or both, are also derived from the fundamental pulse. Calibrated delays between the initiation pulse and probe pulses provide time resolution of the processes occurring in the sample.

Single-pulse measurements are preferable to those in which many pulses are used, regardless of whether the pulses are from the same or different pulse trains, since pulse characteristics such as energy, time and frequency widths, and the pulse substructure vary not only from one train to the next but within a single train as well. For these reasons we usually employ the echelon technique (*5*) (stepped optical delay) whereby it is possible to record the complete time infor-

Dr. Rentzepis is head of the Physical and Inorganic Chemistry Research Department, Bell Laboratories, Murray Hill, New Jersey 07974. Dr. Busch is assistant professor of chemistry at the University of Colorado, Boulder 80309, and is currently an Albert P. Sloan research fellow.

mation in a single experiment. Thus all of the measured results pertain to the same initial excitation conditions. The addition of a spectrograph to the configuration allows the complete time and wavelength characteristics, that is, time-resolved absorption or emission spectra, to be obtained with a single laser pulse. The use of continuum (6) pulses with a duration of a few picoseconds has made it convenient to record broadband absorption spectra and, when used in conjunction with the echelon technique, provides a powerful means for obtaining time-resolved absorption and emission data over an extended spectral region. An example of a two-dimensional spectrum recorded from a single picosecond pulse is shown in Fig. 2. The ordinate shows the time information impressed upon the probe pulse by the echelon, and the abscissa displays wavelength as dispersed and imaged by the grating spectrograph.

Special data handling and analysis procedures are required to deal with the enormous amount of information contained in spectra such as Fig. 2. At present, we use television cameras for direct recording of the two-dimensional spectra in electronic form. This procedure facilitates the immediate processing of the data by an on-line computer system. An example of a computer display of analyzed data appears in Fig. 3, which is a three-dimensional plot of transmitted light intensity versus time and wavelength from an experiment on the vibrational relaxation of a nonheme protein (7).

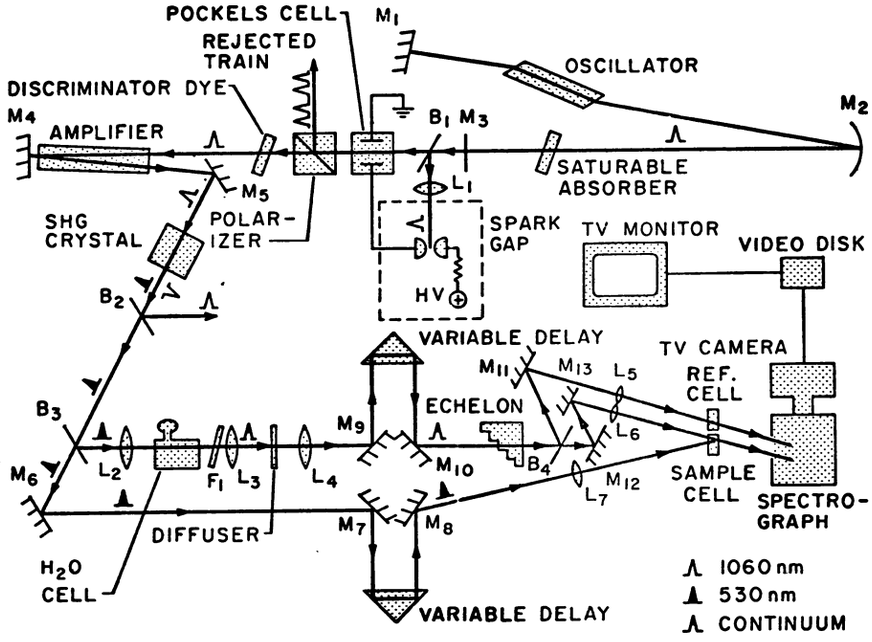

Fig. 1. The experimental configuration used in typical single-pulse picosecond absorption spectroscopy experiments. The train of picosecond 1060-nm pulses produced in the laser oscillator is passed into the single-pulse selector consisting of Pockels cell and polarizer. After amplification, the single pulse generates a second harmonic pulse (530 nm) which may be further frequency-shifted or used directly as the experimental excitation pulse. Light split from the 530-nm pulse at B_3 produces a continuum in the H_2O cell. The continuum pulse is dispersed in time by the echelon and is used to probe the perturbation introduced in the sample cell by the excitation pulse. Time-resolved spectra are recorded by TV camera and video disk. Mirrors, beam splitters, lenses, and filters are designated by the symbols *M*, *B*, *L*, and *F*, respectively; *SHG* crystal, second harmonic generating crystal; *HV*, high voltage.

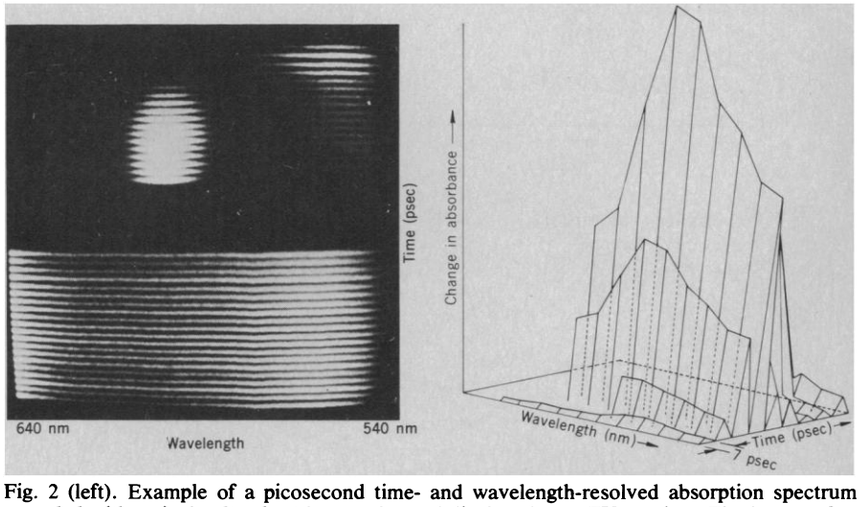

Fig. 2 (left). Example of a picosecond time- and wavelength-resolved absorption spectrum recorded with a single ultrashort laser pulse and displayed on a TV monitor. The lower reference spectrum, recorded as a set of bright horizontal bars, is used in conjunction with the upper spectrum to calculate the fraction of light transmitted by the sample. In the upper spectrum each horizontal bar, or segment, is a full absorption spectrum which is separated in time from adjacent segments by 4 psec. These results were obtained from an investigation of energy transfer between the dyes malachite green and DODCI. At the earliest times (upper right corner), the high-energy tail of the absorption band of malachite green is seen to bleach. This is followed by a rapid recovery of absorption and the appearance of excitation in DODCI, as evidenced by the gradual increase in stimulated emission intensity at 605 nm corresponding to the DODCI emission band. Fig. 3 (right). Simultaneous three-dimensional display of the time-dependent spectrum of a nonheme protein excited by a single 5-psec pulse. The displayed spectrum shows a histogram of the wavelength (*x*-axis); the time evolution (*y*-axis) is shown as a function of intensity (*z*-axis). The time element was provided by a stepped-delay echelon, the wavelength resolution by a 0.75-meter McPherson monochromator recorded by a two-dimensional vidicon and analyzed by a Nova computer.

Laser Pulse Interactions with Absorbing Molecules

Picosecond experiments generally involve the propagation of intense light pulses through an absorbing medium. Since pulse power densities can approach several billion watts per square centimeter, the response of the absorbing system may be qualitatively different from that predicted from a linear extrapolation of behavior at much lower light intensities. A detailed understanding of the nonlinear absorption and emission characteristics of molecules under high-power, ultrashort pulse conditions is important for the proper prediction and interpretation of experimental results obtained from picosecond spectroscopy.

To this end we have developed a model (8) which predicts the temporal behavior of molecular systems during the transmission of intense picosecond light pulses.

To ensure that the model can adequately describe systems within nonlinear regimes, we applied it to the performance of mode-locking and saturable dyes, which respond to irradiation in a highly nonlinear manner, even at moderate power densities (1 to 100 megawatts per square centimeter). Such dyes provide a demanding test for model evaluation.

In most earlier models for the performance of saturable absorbing dyes, it was customary to consider the dye as a simple system with two discrete energy levels. In our model the molecular system is treated in terms of two homogeneously broadened energy levels (*9*) with the result that stimulated emission becomes an important deactivation mechanism for the excited state. This aspect of the model permits photophysical behavior to be characterized in nonlinear regimes. Related nonbroadened four-level models have been treated by Lessing *et al.* (*10*) and Lin *et al.* (*11*) to explain the observation of intensity-dependent fluorescence lifetimes in laser dyes.

We compute a prediction for the response of a sample to irradiation by pulses with a duration of a few picoseconds as a function of time by segmenting the system into units which behave linearly. The appropriate rate equations are integrated on a digital computer. An extremely important aspect of this treatment is that the time-dependent results of picosecond spectroscopy experiments may be extracted directly from the computation because molecular populations are monitored explicitly as functions of time.

An example of the predicted time dependence of probe pulse transmission at the wavelength of the emission maximum of the mode-locking dye DODCI (3,3′-diethyloxadicarbocyanine iodide) is shown as a function of excitation pulse power in Fig. 4a. Significant amplification of probe light is predicted, and the recovery of the dye substantially to its original state occurs on a picosecond time scale. These results are significantly different from the characteristics that would be predicted by the nonbroadened two-level model; this model would not predict gain, and the recovery time would be governed by the excited state lifetime (1.2 nsec) (*12*) of DODCI. The results of experimental measurements on a $2.5 \times 10^{-4}M$ solution of DODCI in ethanol with pulses of $\sim 5 \times 10^{9}$ watts per square centimeter (see Fig. 4b) compare favorably with the predictions in Fig. 4a.

The power and concentration dependences for pulse transmission as predicted from the model are shown in Fig. 4c. These results show reasonable agreement with the experimental data (Fig. 4d). The results are somewhat surprising since one might expect the position of maximum gain to continue to shift to higher concentrations as the excitation pulse power is increased. The qualitative features of the experimental and model curves are in excellent agreement. We expect to make quantitative comparisons as the model is refined.

Two noteworthy predictions are made by the homogeneously broadened two-level model for saturable absorbers used as bleachable filters and shutters. The first is that the greatest dynamic bleaching range is not always achieved at the wavelength of maximum ground state absorption, as is usually assumed, but rather at the wavelength at which the sum of the absorption coefficient of the ground state and the stimulated emission coefficient of the excited state is a maximum. For small Stokes's shifts between absorption and emission, this wavelength will lie midway between the wavelengths of the maxima for the two processes.

The second prediction pertains to applications in which highly concentrated solutions of saturable absorbers are used in bleachable filters to obtain strong discrimination between high- and low-intensity pulses. The homogeneously broadened two-level model predicts that much higher intensities are required to bleach the dye than would be predicted with a simple two-level model because amplified spontaneous emission speeds the return of molecules to the ground state and thereby competes with the bleaching process. The amplified spontaneous emission increases rapidly with concentration and excitation powers and

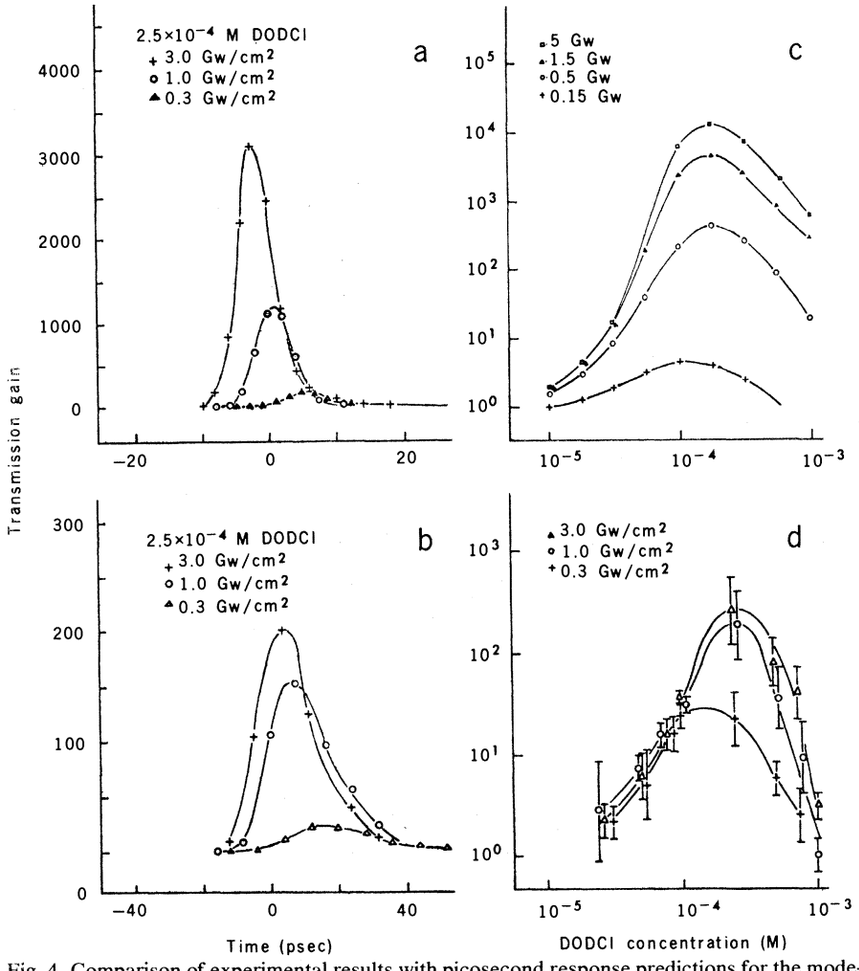

Fig. 4. Comparison of experimental results with picosecond response predictions for the mode-locking dye DODCI, obtained from a nonlinear model described in the text. (a) Calculated time dependence of probe transmission for three different excitation pulse powers. (b) Experimentally measured time dependence for comparison with (a). (c) Calculated dependence of probe light transmission on dye concentration and excitation pulse power density. (d) Experimentally measured results for conditions similar to those used in calculations of (c). In each graph, a methanol solution (2-mm cell) is excited at 530 nm and the plotted sample transmission is for 605-nm probe light. Transmissions greater than unity imply amplification. The predictions in (a) and (c) are seen to be qualitatively correct.

becomes the dominant effect at high values of these parameters.

These preliminary modeling results for the dynamics of ultrashort pulse propagation in molecular systems have revealed that nonlinear molecular responses are likely to produce significant effects in many picosecond spectroscopy experiments. In addition, the development of an accurate model which predicts the dependence of the nonlinearities on system parameters should be important in numerous applications such as the optimization of optically actuated shutters and amplifiers, short pulse generation by passive mode-locking, superradiant pulse emission from optically pumped dye solutions, and pulse transmission through long chains of amplifying and absorbing media such as occur in laser-induced fusion experiments.

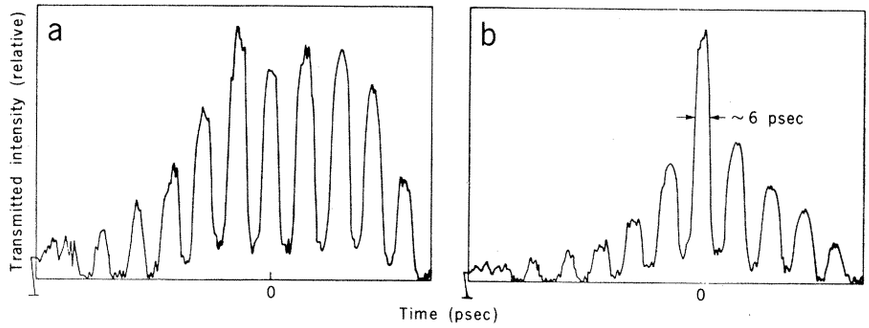

Fig. 5. Histogram of echelon pulses which have traversed through a cell (2-mm path length) containing a solution of sodium and deuterated ammonia. The intersegment separation is 6 psec, and the wavelength is 1100 nm. (a) Transmitted echelon segments without excitation; (b) same as (a) with excitation occurring at time $t = 0$ segment.

Dynamics of Electrons in Fluids

Picosecond spectroscopy has been applied to examining the nature of solvated electron states in liquids (*13*). Studies of the dynamics of the localization of quasi-free electrons in water (*13*) led to the observation of an initial species in about 0.5 psec, and this species relaxes to a new state in less than 4 psec. These results were interpreted in terms of the relaxation of long-range polar interactions, followed by local relaxation of the first coordination layer about the localized electron.

More recently Kenney-Wallace and Jonah used pulsed radiolysis techniques to study the solvation process of free electrons in alcohols (*14*). They observed an initial rapid trapping followed by a slower relaxation process in the range of 18 to 50 psec which they attributed to the rotation times of solvent molecules that were not hydrogen-bonded. The earliest stages of trapping were masked by the 30-psec width of their radiolysis pulse, and thus comparison of their results with those in water (*13*) is difficult.

Recent work by Huppert *et al.* (*15*) was concerned with characterizing the $1s \rightarrow 2p$ transition and excited state lifetime of localized electrons in liquid ammonia. The recovery from the excited state was faster than could be directly resolved, and thus an increase in transmission or bleaching of the absorption (see Fig. 5) during the actual passage of the intense excitation pulse was all that could be detected. On the basis of the extent to which the absorption would be bleached by a pulse of measured intensity, the excited state was estimated to have a lifetime of 2×10^{-13} seconds. Since the entire absorption band in the range from 850 to 1100 nanometers was found to bleach simultaneously and proportionately within the resolution of the measurements, Huppert *et al.* concluded that the band is homogeneously broadened. Hence the width of the transition band is determined by relaxation phenomena rather than by a variation in the local environments seen by electrons.

Photodynamics in Triphenylmethane Dyes

Two recent studies have dealt with fast relaxation in the triphenylmethane dyes crystal violet (*16*) and malachite green (*17*). In each case, lifetimes were measured as a function of solvent viscosity and results were correlated with a model proposed by Förster and Hoffman (*18*). The model assumes that deactivation occurs by rotation of the phenyl rings to a new equilibrium geometry and that there is a slowing of the rotation in viscous solution; the model thus accounts for the dependence of lifetime on solvent viscosity.

In each of these studies different functional forms for the viscosity dependence were determined. In addition, neither of the decays observed were simple exponentials. Magde and Windsor (*16*) fitted their data to a nonexponential function whereas Ippen *et al.* (*17*) interpreted their results at higher viscosities to be composed of two exponentials. The differences in observations could be due to the structural difference between the dyes (a para amino group on one of the phenyl rings in crystal violet is missing in malachite green). Both Magde and Windsor and Ippen *et al.* concluded that the time-resolved results are not in complete agreement with the quantum yield data of Förster and Hoffman. Ippen *et al.* (*17*) noted that a more sophisticated model may be required to describe the system.

In the past year, we have become involved in the problem from a different perspective. In the study of the photodynamics of a number of acid-base indicator dyes, we noted that virtually all of the indicators with the triphenylmethane structure displayed closely related transient bleaching behavior. Our results at high powers are quite similar to those of Ippen *et al.* (*17*). However, we observed what appears to be a two-component decay (two different slopes after excitation) at all viscosities (see Fig. 6). In addition, we did not observe a significant lifetime change for the shortest decay component as the viscosity varied. But the decay characteristics appear to be concentration- and power-dependent, and thus nonlinear effects may be contributing to all of the above results.

The capability of these triphenylmethane dyes to participate in acid-base reactions such as proton transfer may be reflected in the decay data. It is frequently observed (*19*) that excited state pK_a values (the negative logarithm of the dissociation constant) can differ significantly from ground state values. Thus a rapid proton transfer may occur within the excited state, perhaps even providing the radiationless pathway for return to the ground state. Our data suggest that the bleached state of the dye may actually be a nonabsorbing ground state (or possibly a triplet) form of the molecule since stimulated emission from this state is not observed. It might be asked whether we would expect to see emission from a short-lived singlet state; however, we observed intense stimulated emission from dyes with comparable excited state lifetimes, for example, the mode-locking dye EK 9860 which has a measured (*20*) ground state recovery time of ~ 7 psec. For measurements of this type, the advantage of probing the entire spectral

region in a single laser shot with a picosecond continuum becomes apparent.

Confirmation of the nonabsorbing species in the picosecond experiments as either a ground state or a triplet molecule could explain the disagreement between the transient lifetime measurements (*16, 17*) and the earlier fluorescence quantum yield data (*18*). Independent of the nature of the electronic state of the observed transient (or transients if the decay indeed has two components), the species and its generation and decay may involve the process of proton transfer.

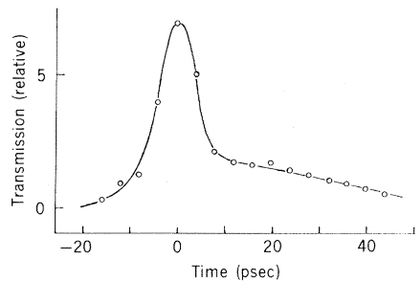

Fig. 6. Picosecond time-resolved bleaching of the triphenylmethane dye crystal violet in methanol solution ($2 \times 10^{-4}M$, 2-mm cell). The dye is excited by an intense 530-nm ultrashort pulse and probed with 570-nm continuum light. Under similar conditions, virtually all triphenylmethane dyes tested exhibited corresponding two-component decays in methanol, ethanol, and glycerin. The detailed shapes of the decays were power- and concentration-dependent, and monotonic decays that appear to be simple exponentials were observed at low excitation powers.

Photochemistry in Biological Systems

In the past few years the techniques of picosecond spectroscopy have been used as effective probes to elucidate primary events in vision and photosynthesis. In the earliest applications by Busch *et al.* in rhodopsin (*21*) and Netzel *et al.* in bacteriochlorophyll (*22*), the kinetics of the initial steps in the photochemical reactive chains were determined. The establishment of time scales for the occurrence of explicit events by direct measurement was an important step toward the determination of reaction mechanisms in these systems. However, perhaps even more meaningful was the demonstration that useful and detailed information could be obtained about picosecond biological processes. Since then, applications have become increasingly more sophisticated and the integration of picosecond spectroscopic techniques with those of electrochemistry and electron paramagnetic resonance (EPR) spectroscopy has led to significant advancements in our understanding of the physical chemistry involved at early stages in photosynthesis. Some of the information that has been obtained is summarized below.

Bacteriochlorophyll Reaction Centers

The reaction centers of the photosynthetic bacterium *Rhodopseudomonas sphaeroides* are known to contain several chemical constituents, including a bacteriochlorophyll dimer, designated $(BChl)_2$, that absorbs at 865 and 605 nm, two bacteriochlorophylls (BChl) absorbing at 800 and 595 nm, two bacteriopheophytins (BPh) absorbing at 760 and ~ 535 nm, and an iron in association with a quinone (QFe). Upon light absorption, the $(BChl)_2$ is oxidized to $(BChl)_2^+$, which results in an EPR signal with a g factor of 2.0026 accompanied by the bleaching of the absorption bands at 865 and 605 nm. Thus the $(BChl)_2$ has been called the primary electron donor. Since the reduction of QFe is a result of the absorption of light, this species has been called the primary electron acceptor. Evidence regarding the roles of the other chemical constituents in reaction centers has only recently emerged.

Netzel *et al.* (*22*) observed that excitation of reaction centers in BChl with a picosecond pulse of light at 530 nm produced bleaching of the absorption band at 865 nm within 10 psec. Since the 535-nm band has generally been attributed to BPh and the 865-nm band is thought to be due to absorption by $(BChl)_2$, this observation is consistent with a rapid transfer of excitation between BPh and $(BChl)_2$, which would require a high degree of interaction between the two chromophores. In addition, the observation established that excitation at 530 nm, which is readily available from mode-locked neodymium glass lasers (being produced with high efficiency by second harmonic generation), was capable of initiating the normal photosynthetic reaction in a non-rate-limiting manner.

These observations were followed by the measurement of picosecond carotenoid band shifts (*23*) in *Rps. sphaeroides* mutant Ga chromatophores (see Fig. 7). Since the carotenoids have only very weak absorption at the 530-nm excitation wavelength, the band shifts were interpreted as arising from an interaction of the carotenoids with a strong dipolar field induced by a proposed diradical state ($BChl^+$–$BChl^-$) which may be responsible for the EPR spectra observed in reaction centers at low temperatures.

This interpretation was supported by additional evidence. (i) The shifts are similar to carotenoid band shifts induced by alterations in the membrane field. (ii) The shifts are not observed in the carotenoid-free mutant *Rps. sphaeroides* R26. (iii) The response is eliminated when the reaction centers are oxidized with ferricyanide to produce $(BChl)_2^+$, and thus formation of ($BChl^+$–$BChl^-$) is prevented. (iv) The electron transfer process is not involved since its inhibition by the addition of dithionite does not affect the picosecond band-shift response.

The rapidity of the shift further implicates the involvement of the reaction center species that is produced prior to electron transfer (see below). The magnitude of the absorbance changes ($\Delta A/A > 0.2$) indicates that a large portion of the carotenoids is affected and that these species must be bound close to, if not directly to, the reaction center protein.

Independent picosecond experiments by two groups (*24, 25*) demonstrated that electron transfer to the primary electron acceptor does not occur immediately on the picosecond time scale in *Rps. sphaeroides* R26. Transient spectra were recorded which revealed a substantial increase in absorption throughout the spectral region from 500 to 700 nm except for the two regions of bleaching at 540 and 600 nm. The bleaching was attributed by Kaufmann *et al.* (*24*) to the disappearance of BPh (540 nm) and BChl (600 nm). The absorption changes disappear on a time scale of 150 to 250 psec (*24, 25*) (see Fig. 8a), indicating a decay of the intermediate to the oxidized dimer $(BChl)_2^+$.

Kaufmann *et al.* observed (*24*) that, when transfer of the electron to the primary electron acceptor is blocked by prior chemical reduction of the reaction center, the lifetime of the intermediate is greatly increased (see Fig. 8b) so that the spectrum does not decay significantly on the picosecond time scale. Kaufmann *et al.* thus concluded that the intermediate was the same as one that had been observed by Parson *et al.* (*26*), using nanosecond flash techniques.

The observation that the decay of the first resolvable transient species could be essentially blocked by chemical reduction suggested that only one intermediate with a significant lifetime was produced prior to electron transfer. That it is indeed the quinone that is reduced within the reaction center by the above chemical treatment and thus that the quinone is in fact a primary electron acceptor was demonstrated in very recent experiments by Kaufmann *et al.* (*27*). They showed that complete removal of the quinone

from the reaction centers by chemical extraction produced the same degree of lifetime increase as is produced by reduction. Furthermore, when quinone is added to the extracted reaction centers, the recovery characteristics of the transient intermediate revert to those observed in untreated reaction centers.

The implication of the participation of BPh and BChl in the transient intermediate state prior to electron transfer, arising from transient bleaching of the bands at 540 and 600 nm, has led to further experiments and speculation on the nature of the transient intermediate. Dutton *et al.* (*28*) have investigated the picosecond kinetics of the 1250-nm band observed in oxidized *Rps. sphaeroides* reaction centers. Since the band is not apparent in oxidized BChl in organic solutions, Dutton *et al.* assumed it to be unique to the oxidized $(BChl)_2^+$ species in reaction centers. The band appeared within 10 psec (Fig. 9) after excitation by a picosecond laser pulse at 530 nm. Dutton *et al.* thus concluded that $(BChl)_2^+$ is formed immediately, rather than upon decay of the transient species [designated P^F by Parson *et al.* (*26*)] and transfer of the electron to the primary electron acceptor. These results can be explained in terms of the prompt formation of $(BChl)_2^+$ in the species P^F which is a composite of the oxidized dimer and the reduced form of some other reaction center constituent, I (*28*). Primary electron transfer would then occur when the electron is transferred from I^- to the primary electron acceptor X (which is most likely the quinone); thus I may be considered to act as an electron transfer intermediary between the $(BChl)_2$ and X in a manner represented schematically by the following ferrocytochrome sequence:

Ferrocyt C_2 (BChl–BChl I)X
↓ $h\nu$
Ferrocyt C_2 (BChl*BChl I)X
↓ ≤ 10 psec
Ferrocyt C_2 (BChl$^+$BChl I$^-$)X
↓ 100 to 150 psec
Ferrocyt C_2 (BChl$^+$BChl I)X$^-$
↓ 20 μsec
Ferrocyt C_2^+ (BChl–BChl I)X$^-$
↓
Recombination by way of cyclic electron transfer system

in which the initially excited species (signified by *) may or may not be the same as the first spectroscopically observed species, which Dutton *et al.* (*28*) proposed involves the species I^-.

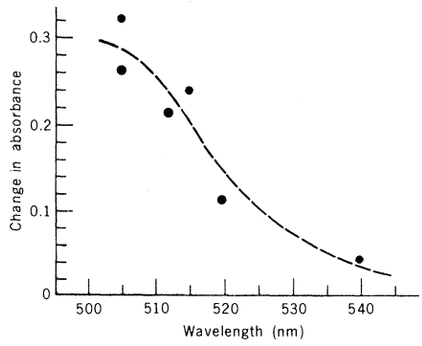

Fig. 7. Partial spectrum of the absorbance changes in *Rps. sphaeroides* Ga chromatophores measured 20 psec after excitation. The sample was suspended in 10 m*M* tris-HCl buffer; *p*H 8.0; BChl concentration, 150 μM; path length, 5 mm; spectral resolution, 2.4 nm; temperature, 22°C.

Possibilities for I^- were considered by Dutton *et al.* (*28*). Although they did not rule out $BChl^-$, they favored BPh^- as the most likely candidate since it was more in accord with a number of features of the spectral data. Recent results (*29*) indicate that it is possible to block the formation of the $(BChl)_2^+$ by prior reduction of I.

Plant Chloroplast Photosystems

Several studies have been carried out on the chlorophyll present in plant chloroplasts (*30–33*). The existence of two photosystems in the chloroplasts indicates that plant photosystems are more complex than bacterial systems. Therefore, it is expected that the interpretation of results in plant systems will be more difficult. It is also not clear that significant correspondence will exist between the mechanisms and kinetics discovered in the two chlorophyll systems; however, it seems likely that insight gained from bacteriochlorophyll systems will aid in development of a viable model for plant photosynthesis.

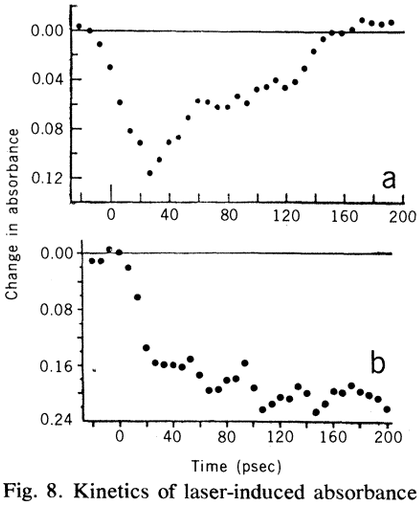

Fig. 8. Kinetics of laser-induced absorbance changes in *Rps. sphaeroides* R26 reaction centers at 540 nm: (a) E_h (oxidation-reduction potential) ~ +200 millivolts; (b) E_h < −200 millivolts.

Most of the picosecond studies on plant photosynthesis thus far have consisted of measurements of fluorescence decays in isolated chloroplasts or in chlorophyll solutions. In an early report of measurements on escarole and spinach chloroplasts, Seibert and Alfano observed two separate maxima in fluorescence decay curves measured at 685 nm (*30*); it was suggested that the maxima, which occur at about 10 to 15 psec (decay time ~ 10 psec) and 90 psec (decay time ~ 210 psec in spinach and 320 psec in escarole chloroplasts) after excitation, might result from separate emissions of photosystem I and photosystem II, respectively. Seibert and Alfano speculated that the 90-psec delay in the emission maximum of photosystem II could be due to initial absorption by accessory pigments and carotenoids, followed by energy transfer to chlorophyll a of photosystem II. The results were compared (*30*) to several kinetic models, two of which were capable of yielding two maxima in the decays.

In more recent measurements of fluorescence decays in spinach chloroplasts (*31*) prepared by a different technique, the 10-psec decay time and the maximum in the decay curve at 90 psec were not observed. Lifetimes of 60 and 200 psec were reported for photosystem I and photosystem II, respectively. The discrepancy in the early time behavior for the two studies was attributed to differences in sample preparation.

For some experimental conditions, dye modeling calculations (mentioned above) can be used to predict curves of the same general shape as reported in the earlier chloroplast measurements. The situation arises in the calculations (*8*) under conditions of high concentration and intermediate excitation intensity. The initial rapid decay occurs as a result of amplified spontaneous fluorescence, and the second maximum arises from the amplification of reflections from the cell windows. Aqueous solutions in a 1-centimeter cell with a 1-millimeter window can produce the second maximum near 100 psec.

Shapiro *et al.* (*32*) showed that the very short lifetimes of fluorescence decays obtained for living plant cells could be due to concentration quench-

ing. Solutions of chlorophyll a and chlorophyll b prepared at the high concentrations known to be present in living cells exhibited lifetimes in the same range as observed in cells. The concentration dependence of the lifetime was in good agreement with the transfer of excitation by dipole-dipole interactions according to the Förster model of energy transfer (*33*).

In other quenching experiments on solutions of chlorophyll, Huppert *et al.* (*34*) measured the rate of quenching of the first excited singlet state of chlorophyll a by quinone. The possible direct transfer of an electron from photoexcited chlorophyll a to quinone, as the primary process in photosystem II, was investigated by monitoring for evidence of production of Chl^+. The rate of quenching of the excited singlet of chlorophyll a was followed by the use of time-resolved absorption techniques. Bleaching of the ground state band at 665 nm and new transient absorption bands in the region of 460 to 550 and 800 to 830 nm appeared within 10 psec and remained after 0.5 nsec in the absence of quinone. The transient spectra were observed to decay with a lifetime of about 400 psec at a quinone concentration of 0.16*M*; however, no evidence for the production of Chl^+ was obtained. Huppert *et al.* concluded that the electron transfer does not occur in solution.

Recent measurements by Campillo *et al.* (*35*) of the excitation intensity dependence of quantum yields of fluorescence from chloroplasts indicates that an exciton-exciton annihilation mechanism may be operative at high excitation intensity. They concluded that earlier measurements of lifetimes in chloroplasts were most likely affected by this process, resulting in shortened lifetimes.

A number of additional nonlinear effects could become important at high intensity, including saturation of absorption and amplified spontaneous emission. Since the latter will in general be anisotropic, it can affect measurements of quantum yields and also can reduce lifetimes.

Primary Processes in Vision

The earliest application of the techniques of picosecond spectroscopy to photochemical processes in biological systems involved studies of the primary photochemical events in bovine rhodopsin (*21*). Since that time, most of the biologically oriented work has been in photosynthetic systems involving chlorophyll. Only very recently (*36, 37*) has attention again been directed toward the visual pigments.

One study (*36*) was carried out in the retinal-containing bacterial system *Halobacterium halobium*. The long conjugated polyene retinal is the same light-absorbing chromophore as that found in rhodopsin, the visual pigment in vertebrates. Bacteriorhodopsin is used by the bacterium as a means of utilizing photon energy in the synthesis of adenosine triphosphate. A number of intermediates in the photoreaction sequence of light-adapted bacteriorhodopsin have been characterized.

There are similarities between the photoreactions of bovine rhodopsin and bacteriorhodopsin. In each case the absorption of light produces a transient species which appears within the resolution time afforded by the picosecond excitation and monitoring pulses. The species is characterized by an absorption band which is red-shifted with respect to the normal ground state absorption. The band persists for a period that is long compared to the time scale of the picosecond measurements. The results of measurements utilizing techniques with lower time resolution indicate that the lifetime is approximately 30 nsec for the initial intermediate in bovine rhodopsin (*21*), in contrast to the case for the bacteriorhodopsin intermediate which has a lifetime of microseconds at physiological temperatures (35° to 40°C). Moreover, bacteriorhodopsin returns to its initial state without any additional energy input, whereas the restoration of bovine rhodopsin requires endothermic dark-reaction steps.

Since the final stages of the visual process are known to involve the all-*trans* form of the retinal molecule (the 11-*cis* form prevails before light absorption), it has been proposed (*38*), and it is generally accepted, that the primary step involves a *cis-trans* isomerization. However, because of the extreme speed with which the first intermediate is produced, it has been argued (*21*) that there is insufficient time for the required molecular motion. If there is a correspondence between the two systems, then the results that have been obtained in the bacteriorhodopsin study provide evidence that *cis-trans* isomerization is not occurring in this step (the initial state of retinal in bacteriorhodopsin is already the all-*trans* configuration prior to light absorption).

An alternative initial step involves an electron transfer between an amino acid residue in the protein and the chromophore. This and other mechanisms are being considered in continuing investigations of each of these pigment systems as well as in several retinyladene Schiff base model compounds (*37*).

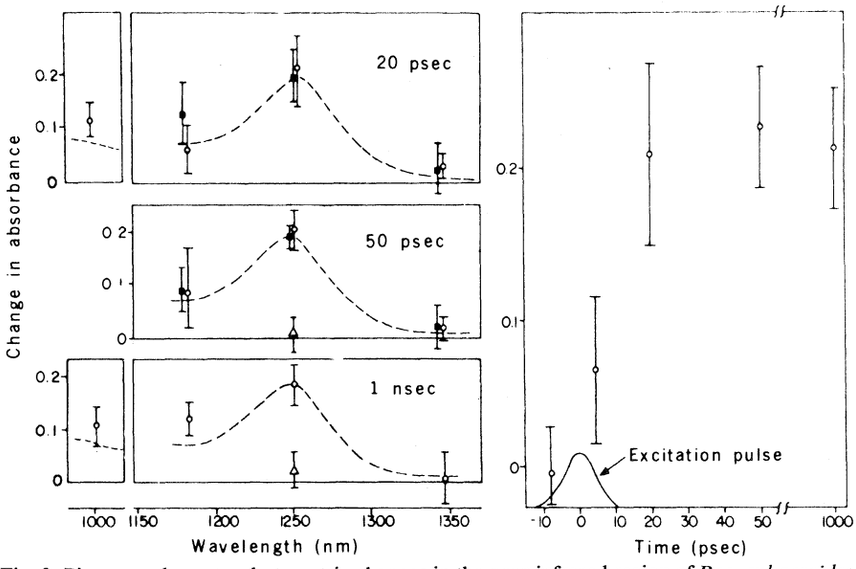

Fig. 9. Picosecond spectrophotometric changes in the near-infrared region of *Rps. sphaeroides* reaction centers. The reaction centers were used and suspended as described in (*28*) and examined in a 2 m*M* anaerobic oxidation-reduction cuvette. The reaction centers were poised at different oxidation-reduction states as follows: In the neutral form, BChl–BChl X (○); in the ferricyanide-oxidized form, $BChl^{+}$–BChl X (△); and with the primary electron acceptor reduced, BChl–BChl X^- (■). The right side of the figure shows points taken at various times before and after the flash at 1250 nm. The left side shows points taken at various wavelengths and times after the flash. Each point is the average of at least four determinations. The error bars represent the mean standard deviation. The laser light used for activation was not saturating.

Summary

The ability to directly measure and evaluate ultrafast processes with unprecedented time resolution and reliability has greatly extended our knowledge about the kinetics of primary processes in chemistry and allied physical and biological sciences. Improvements in the reliability and versatility of picosecond techniques should lead to an increase in the experimental information about basic interactions in atomic and molecular systems.

References and Notes

1. P. M. Rentzepis, *Chem. Phys. Lett.* **2**, 37 (1968).
2. D. Huppert, thesis, Tel-Aviv University, Ramat-Aviv, Israel (1975); _____ and P. M. Rentzepis, in *Molecular Energy Transfer*, R. D. Levine and J. Jortner, Eds. (Wiley, New York, 1975), p. 278.
3. K. B. Eisenthal, *Acc. Chem. Res.* **8**, 118 (1975); K. J. Kaufmann and P. M. Rentzepis, *ibid.*, p. 407; A. Lauberau and W. Kaiser, *Annu. Rev. Phys. Chem.* **26**, 83 (1975); R. R. Alfano and S. L. Shapiro, *Phys. Today* **1975**, 30 (July 1975).
4. P. W. Smith, M. A. Duguay, E. P. Ippen, *Prog. Quantum Electron.* **3**, 1 (1974).
5. M. R. Topp, P. M. Rentzepis, R. P. Jones, *J. Appl. Phys.* **42**, 3451 (1971).
6. R. R. Alfano and S. L. Shapiro, *Phys. Rev. Lett.* **24**, 584 (1970); G. E. Busch, P. M. Rentzepis, R. P. Jones, *Chem. Phys. Lett.* **18**, 178 (1973).
7. D. Huppert, K. Straub, E. O. Degenkolb, P. M. Rentzepis, in preparation.
8. K. S. Greve and G. E. Busch, in preparation.
9. C. V. Shank, *Rev. Mod. Phys.* **47**, 649 (1975).
10. H. E. Lessing, E. Lippert, W. Rapp, *Chem. Phys. Lett.* **7**, 247 (1970).
11. C. Lin, T. K. Gustafson, A. Dienes, *Opt. Commun.* **8**, 210 (1973).
12. D. N. Dempster, T. Morrow, R. Rankin, G. F. Thompson, *J. Chem. Soc. Faraday Trans. 2* **68**, 1479 (1972).
13. P. M. Rentzepis, R. P. Jones, J. Jortner, *J. Chem. Phys.* **54**, 766 (1973).
14. G. A. Kenney-Wallace and C. D. Jonah, *Chem. Phys. Lett.* **39**, 596 (1976).
15. D. Huppert, W. S. Struve, P. M. Rentzepis, J. Jortner, *J. Chem. Phys.* **63**, 1205 (1973).
16. D. Magde and M. W. Windsor, *Chem. Phys. Lett.* **24**, 144 (1974).
17. E. P. Ippen, C. V. Shank, A. Bergman, *ibid.* **38**, 611 (1976).
18. T. Förster and G. Hoffman, *Z. Phys. Chem. Neue Folge* **75**, 63 (1971).
19. J. F. Ireland and P. A. H. Wyatt, *Adv. Phys. Org. Chem.* **12**, 131 (1976).
20. D. von der Linde and K. F. Rodgers, *IEEE J. Quantum Electron.* **QE-9**, 960 (1973).
21. G. E. Busch, M. L. Applebury, A. Lamola, P. M. Rentzepis, *Proc. Natl. Acad. Sci. U.S.A.* **69**, 2802 (1972).
22. T. L. Netzel, P. M. Rentzepis, J. Leigh, *Science* **182**, 238 (1973).
23. J. S. Leigh, Jr., T. L. Netzel, P. L. Dutton, P. M. Rentzepis, *FEBS Lett.* **48**, 136 (1974).
24. K. J. Kaufmann, P. L. Dutton, T. L. Netzel, J. S. Leigh, P. M. Rentzepis, *Science* **188**, 1301 (1975).
25. M. G. Rockley, M. M. Windsor, R. J. Cogdell, W. W. Parson, *Proc. Natl. Acad. Sci. U.S.A.* **72**, 2251 (1975).
26. W. W. Parson, R. K. Clayton, R. J. Cogdell, *Biochim. Biophys. Acta* **387**, 265 (1975).
27. K. J. Kaufmann, K. M. Petty, P. L. Dutton, P. M. Rentzepis, *Biochem. Biophys. Res. Commun.* **70**, 839 (1976).
28. P. L. Dutton, K. J. Kaufmann, B. Chance, P. M. Rentzepis, *FEBS Lett.* **60**, 275 (1975).
29. T. L. Netzel, P. L. Dutton, P. M. Rentzepis, in preparation.
30. M. Seibert and R. R. Alfano, *Biophys. J.* **14**, 269 (1974).
31. W. Yu, P. P. Ho, R. R. Alfano, M. Seibert, *Biochim. Biophys. Acta* **387**, 159 (1975).
32. S. L. Shapiro, V. H. Kollman, A. J. Campillo, *FEBS Lett.* **54**, 358 (1975).
33. See, for example, J. B. Birks, *Photophysics of Aromatic Molecules* (Wiley-Interscience, New York, 1970), pp. 567–590.
34. D. Huppert, P. M. Rentzepis, G. Tollin, *Biochim. Biophys. Acta* **440**, 356 (1976).
35. A. J. Campillo, S. L. Shapiro, V. H. Kollman, K. R. Winn, R. C. Hyer, *Biophys. J.* **16**, 93 (1976).
36. K. J. Kaufmann, P. M. Rentzepis, W. Stoeckenius, A. Lewis, *Biochem. Biophys. Res. Commun.* **68**, 1109 (1976).
37. D. Huppert, P. M. Rentzepis, D. Kliger, *Photochem. Photobiol.*, in press.
38. G. Wald, *Science* **162**, 230 (1968).
39. We thank Drs. P. L. Dutton, D. Huppert, and K. Kaufmann and K. S. Greve, G. Olson, and R. Ito for their many helpful contributions and discussions.

Cooperative Computation of Stereo Disparity

A cooperative algorithm is derived for extracting disparity information from stereo image pairs.

D. Marr and T. Poggio

Perhaps one of the most striking differences between a brain and today's computers is the amount of "wiring." In a digital computer the ratio of connections to components is about 3, whereas for the mammalian cortex it lies between 10 and 10,000 (*1*).

Although this fact points to a clear structural difference between the two, this distinction is not fundamental to the nature of the information processing that each accomplishes, merely to the particulars of how each does it. In Chomsky's terms (*2*), this difference affects theories of performance but not theories of competence, because the nature of a computation that is carried out by a machine or a nervous system depends only on a problem to be solved, not on the available hardware (*3*). Nevertheless, one can expect a nervous system and a digital computer to use different types of algorithm, even when performing the same underlying computation. Algorithms with a parallel structure, requiring many simultaneous local operations on large data arrays, are expensive for today's computers but probably well-suited to the highly interactive organization of nervous systems.

The class of parallel algorithms includes an interesting and not precisely definable subclass which we may call cooperative algorithms (*3*). Such algorithms operate on many "input" elements and reach a global organization by way of local, interactive constraints. The term "cooperative" refers to the way in which local operations appear to cooperate in forming global order in a well-regulated manner. Cooperative phenomena are well known in physics (*4, 5*), and it has been proposed that they may play an important role in biological systems as well (*6–10*). One of the earliest suggestions along these lines was made by Julesz (*11*), who maintains that stereoscopic fusion is a cooperative process. His model, which consists of an array of dipole magnets with springs coupling the tips of adjacent dipoles, represents a suggestive metaphor for this idea. Besides its biological relevance, the extraction of stereoscopic information is an important and yet unsolved problem in visual information processing (*12*). For this reason—and also as a case in point—we describe a cooperative algorithm for this computation.

In this article, we (i) analyze the computational structure of the stereo-disparity problem, stating the goal of the computation and characterizing the associated local constraints; (ii) describe a cooperative algorithm that implements this computation; and (iii) exhibit its performance on random-dot stereograms. Although the problem addressed here is not directly related to the question of

D. Marr is at the Artificial Intelligence Laboratory, Massachusetts Institute of Technology, Cambridge 02139. T. Poggio is at the Max-Planck Institut für Biologische Kybernetik, 74 Tubingen 1, Spemannstrasse 38, Germany.